


# Tumour catabolism independent of malnutrition and inflammation in upper GI cancer patients revealed by longitudinal metabolomics

Janusz von Renesse<sup>1</sup>, Felix von Bechtolsheim<sup>1</sup>, Sophie Jonas<sup>2</sup>, Lena Seifert<sup>1,3,4</sup>, Tiago C. Alves<sup>2</sup>, Adrian M. Seifert<sup>1,3,4</sup>, Filip Komorek<sup>1</sup>, Guergana Tritchkova<sup>1</sup>, Mario Menschikowski<sup>2</sup>, Ulrich Bork<sup>1</sup>, Ronny Meisterfeld<sup>1</sup>, Marius Distler<sup>1</sup>, Triantafyllos Chavakis<sup>2,3</sup>, Jürgen Weitz<sup>1,3,4</sup>, Alexander M. Funk<sup>2,3†</sup>, Christoph Kahlert<sup>1,3,4†</sup> & Peter Mirtschink<sup>2\*†</sup> 

<sup>1</sup>Department of Visceral, Thoracic and Vascular Surgery, University Hospital Carl Gustav Carus Dresden, Technische Universität Dresden, Dresden, Germany; <sup>2</sup>Institute of Clinical Chemistry and Laboratory Medicine, University Hospital and Faculty of Medicine, Technische Universität Dresden, Dresden, Germany; <sup>3</sup>National Center for Tumor Diseases (NCT), Partner Site Dresden, Dresden, German Cancer Research Center (DKFZ), Heidelberg, Germany; <sup>4</sup>German Cancer Consortium (DKTK), Partner Site Dresden, Dresden, German Cancer Research Center (DKFZ), Heidelberg, Germany

## Abstract

**Background** The detrimental impact of malnutrition and cachexia in cancer patients subjected to surgical resection is well established. However, how systemic and local metabolic alterations in cancer patients impact the serum metabolite signature, thereby leading to cancer-specific differences, is poorly defined. In order to implement metabolomics as a potential tool in clinical diagnostics and disease follow-up, targeted metabolite profiling based on quantitative measurements is essential. We hypothesized that the quantitative metabolic profile assessed by <sup>1</sup>H nuclear magnetic resonance (NMR) spectroscopy can be used to identify cancer-induced catabolism and potentially distinguish between specific tumour entities. Importantly, to prove tumour dependency and assess metabolic normalization, we additionally analysed the metabolome of patients' sera longitudinally post-surgery in order to assess metabolic normalization.

**Methods** Forty two metabolites in sera of patients with tumour entities known to cause malnutrition and cachexia, namely, upper gastrointestinal cancer and pancreatic cancer, as well as sera of healthy controls, were quantified by <sup>1</sup>H NMR spectroscopy.

**Results** Comparing serum metabolites of patients with gastrointestinal cancer with healthy controls and pancreatic cancer patients, we identified at least 15 significantly changed metabolites in each comparison. Principal component and pathway analysis tools showed a catabolic signature in preoperative upper gastrointestinal cancer patients. The most specifically upregulated metabolite group in gastrointestinal cancer patients was ketone bodies (3-hydroxybutyrate,  $P < 0.0001$ ; acetoacetate,  $P < 0.0001$ ; acetone,  $P < 0.0001$ ; false discovery rate [FDR] adjusted). Increased glycerol levels ( $P < 0.0001$ ), increased concentration of the ketogenic amino acid lysine ( $P = 0.03$ ) and a significant correlation of 3-hydroxybutyrate levels with branched-chained amino acids (leucine,  $P = 0.02$ ; isoleucine,  $P = 0.04$  [FDR adjusted]) suggested that ketone body synthesis was driven by lipolysis and amino acid breakdown. Interestingly, the catabolic signature was independent of the body mass index, clinically assessed malnutrition using the nutritional risk screening score, and systemic inflammation assessed by CRP and leukocyte count. Longitudinal measurements and principal component analyses revealed a quick normalization of key metabolic alterations seven days post-surgery, including ketosis.

**Conclusions** Together, the quantitative metabolic profile obtained by <sup>1</sup>H NMR spectroscopy identified a tumour-induced catabolic signature specific to upper gastrointestinal cancer patients and enabled monitoring restoration of metabolic homeostasis after surgery. This approach was critical to identify the obtained metabolic profile as an upper gastrointestinal cancer-specific signature independent of malnutrition and inflammation.

**Keywords** NMR; Gastrointestinal cancer; Metabolic profile; Metabolome; Ketone bodies; 3-Hydroxybutyrate

Received: 8 July 2022; Revised: 1 October 2022; Accepted: 25 October 2022

\*Correspondence to: Peter Mirtschink, Institute of Clinical Chemistry and Laboratory Medicine, University Hospital Carl Gustav Carus, Technische Universität (TU) Dresden, Fetscherstr. 74, 01307 Dresden, Germany. Email: peter.mirtschink@ukdd.de

†Alexander M. Funk, Christoph Kahlert and Peter Mirtschink have contributed equally to this work.

## Introduction

Modern, multimodal oncological therapy, including surgery, chemo- and radiotherapy, has improved outcomes of patients with gastroesophageal cancer in recent years.<sup>1</sup> Nonetheless, gastroesophageal cancer is still a leading cause of cancer-related deaths worldwide.<sup>2</sup> Hence, novel approaches are needed to improve our understanding of disease progression, identify patients at risk and follow-up the post-surgery disease outcome. Studies in various animal models and patients have revealed that gastroesophageal tumours may induce systemic metabolic alterations by a combination of increasing energy expenditure, mechanical food intake obstruction, increased catabolic activity, metabolic dysregulation and systemic inflammation.<sup>3</sup> These disturbances may result in cancer cachexia and malnutrition, which are major contributors to postoperative morbidity and mortality after surgical resection.<sup>4</sup> The prevalence of preoperative malnutrition in gastroesophageal cancer patients ranges from 40% to 60%, and sarcopenia is reported to occur ranging from 6.8% to 79%.<sup>5,6</sup>

Malnutrition is defined by reduced nutrient intake, mainly leading to body fat catabolism but also muscle mass reduction, resulting in overall weight loss. In contrast, cancer cachexia is a pathological process inducing weight loss mainly due to muscle catabolism with or without body fat loss and is accompanied by inflammation.<sup>7</sup> Many studies have shown the deteriorating effect of malnutrition and decreased muscle mass on patients undergoing major surgery due to upper gastrointestinal (upper GI) carcinoma.<sup>8</sup> Cancer cachexia and, in particular, decreased muscle mass and function are associated with poor quality of life and worse patient outcomes.<sup>9</sup> Cancer is believed to induce cachexia by a combination of increasing energy expenditure, mechanical food intake obstruction, increased catabolic activity and metabolic dysregulation, and systemic inflammation.<sup>7</sup> Early preoperative diagnosis and consecutive nutritional intervention before surgery can improve outcomes.<sup>10</sup> To this end, various screening modalities have been developed to identify patients at risk.<sup>11</sup> An established screening tool is the Nutritional Risk Screening score (NRS), which can detect patients at preoperative nutritional risk.<sup>12</sup>

Nevertheless, the NRS and similar screening modalities are based on a partially subjective rating either by a physician or the patient, which can lead to false conclusions regarding the patient's nutritional status. Additionally, clinical evaluation can miss metabolic disturbances preceding clinical manifestation. It is currently difficult to determine which patient subset will develop cancer-induced muscle loss before the onset of severe symptoms. Early identification of patients at risk for catabolic metabolism would allow optimal nutritional classification and support, enabling a shift from reacting to the loss of function towards prevention.<sup>7</sup>

Malnutrition and starvation that require global metabolic adaptations are associated with changes in the metabolic profile.<sup>13</sup> In order to establish serum metabolic profiles as a valuable approach in the clinical routine, absolute quantitative analyses are mandatory to ensure reproducibility and enable calculation of appropriate reference values. Moreover, physiological interpretation of relative metabolite concentrations is limited, as the comparison with known homeostatic levels is impossible. Hence, the present study uses a targeted metabolomics approach by <sup>1</sup>H nuclear magnetic resonance (NMR) spectroscopy and multivariate statistical analysis to measure the concentration of various metabolites in human blood serum samples of patients with upper gastrointestinal (GI) cancer located in the oesophagus or stomach (collectively termed upper GI), healthy controls and pancreatic cancer (PanC) patients in an attempt to identify disease-related metabolite concentration differences.

So far, efforts to identify metabolic alterations in upper GI cancer patients employed solely cross-sectional study designs comparing healthy individuals with diagnosed patients.<sup>14</sup> This approach is not ideal for discriminating between patient-dependent confounding effects and cancer-induced metabolic changes. The metabolome adapts very rapidly to changing environmental conditions, making it particularly suitable for dynamic studies. The problem of high heterogeneity of the metabolome can be circumvented by using longitudinal measurements as an internal control. Therefore, analyses on tumour-induced metabolic alteration should include serum metabolomic profile measurements before tumour resection and longitudinal follow-up postoperatively. Many cross-sectional studies have proven metabolic alteration in cancer patient sera, but longitudinal studies are urgently needed to prove tumour dependency and to assess normalization velocity after resection. Thus, longitudinal sample collection up to 7 days post-surgery was used to test whether the metabolite profile of upper GI cancer patients returns to a normal state and at which time altered metabolites reach physiologic concentrations.

## Methods

### *Human subjects and sample collection*

The study protocol was approved by the Ethics Committee of the *Technische Universität* (IRB number 00001473) Dresden (file number EK-109032022) and was conducted following the Declaration of Helsinki. Written informed consent was obtained from all patients or healthy volunteers before study inclusion. In total, 48 patients with upper GI cancer and 39 patients with pancreatic cancer were included in the study

over the period of November 2018 to September 2019. Moreover, samples from 59 healthy volunteers were analysed. The samples were immediately frozen and stored at  $-80^{\circ}\text{C}$ .

### *NMR sample measurement and analysis*

$^1\text{H}$  NMR spectroscopy measurements were performed according to established protocols.<sup>15</sup> The frozen serum samples were thawed at room temperature for about 30 min before being mixed with phosphate buffer (1:1) to a volume of 600  $\mu\text{L}$ . The resulting mixture was pipetted into the NMR sample tube and immediately prepared for measurement.

All measurements were run on a Bruker 600-MHz Avance III Neo NMR-spectrometer equipped with a BBI Probe and a Bruker SampleJet robot with a cooling system for sample storage at  $4^{\circ}\text{C}$ . The samples were measured at 310 K, and a full quantitative calibration was completed before the measurement. All experiments were completed using the Bruker in vitro diagnostics (IVDr) methods.<sup>15</sup> All data were processed in automation using Bruker TopSpin 4.1.1 and ICON-NMR. Metabolite reports (40 parameters) were obtained using Bruker IVDr B.I. Methods Plasma/Serum Analysis (B.I.Quant-PS, v.2.0.0). Triglycerides and cholesterol concentration were assessed using Bruker Lipoprotein Subclass Analysis (B.I.LISA, v.1.0.0). The analysis was performed on 1D Nuclear Overhauser Spectroscopy experiments (1D NOESY).

### *Statistical analysis*

All statistical analyses were performed using the R statistics environment (version 4.0.1, R Foundation for Statistical Computing, [www.r-project.org](http://www.r-project.org)) using the MetaboAnalystR 3 package. Graphical visualization was performed using GraphPad Prism v8 (GraphPad Software, Inc, La Jolla, CA, USA) and Metaboanalyst 5.0.<sup>16</sup>

Concerning demographical and clinical data, a normal distribution test, a Student's *t*-test, or Kruskal–Wallis test was performed to compare groups accordingly. Categorical variables were summarized as absolute and relative frequencies (percentages) and compared using the  $\chi^2$  test or exact Fischer test, depending on sample size.

For multivariate analyses, a data integrity check was performed. First, to avoid random noise and systematic missingness, we filtered out metabolites with constant or single values across samples. In some samples, metabolite concentrations did not reach the limit of detection; a common observation in metabolomics analyses.<sup>17</sup> Accordingly, we used the recommended minimum imputation default setting of MetaboAnalyst 5.0 for missing value imputation.<sup>18</sup> Dimension reduction and exploratory analysis of identified metabolites were performed using unsupervised principal

component analysis (PCA). orthogonal partial least-squares discriminant analysis (OPLS-DA) was used to identify features driving group separation. To evaluate the importance of specific variables for separation in OPLS-DA, variable importance in projection (VIP) was calculated for every metabolite. Metabolite concentrations were compared using Student's *t*-test for normally distributed and Mann–Whitney *U*-test for non-normally distributed data. Longitudinal metabolic data were analysed by ANOVA, followed by Tukey's multiple comparisons test.

*P* values were adjusted for multiple testing using the false discovery rate (FDR) method. All *P* values were considered statistically significant at a level of less than 0.05.

## **Results**

### *Study design*

A total of 283 serum samples from 48 upper GI cancer patients, 39 PanC patients and 59 healthy controls were available for metabolomic analysis (*Figure 1A*). Blood was collected from enrolled cancer patients immediately before surgery (d0). Further longitudinal samples were collected from upper GI cancer patients on the first (d1), third (d3), and seventh (d7) postoperative days, if possible (*Figure 1A*).

Within the control group of third year medical students 47 were male and 13 female resembling the distribution of the upper GI study group. Of the 48 upper GI patients, 38 were male, and 10 were female, whereas 17 PanC patients were female, and 22 were male. Although both groups had a higher male ratio, the upper GI group had significantly more men. Age and body mass index (BMI) did not differ between groups (Supporting information, *Table S1*). Importantly, there were no differences in the assessment of comorbidities and fitness using the clinically approved scoring system 'Charlson Comorbidity Index' or the 'American Society of Anesthesiologists' (ASA) score. Specific comorbidities were equally distributed between both groups (*Table S1*).

### *Upper GI cancer induces specific metabolic alterations*

This study aimed to identify metabolic alterations induced by cancer located in the upper GI tract. First, we compared preoperative blood draws of upper GI cancer patients with healthy controls to unravel tumour-induced metabolic disturbances. Due to expected confounding effects linked to age differences and pre-existing diseases in the upper GI group, we further confirmed our findings with an additional control group of PanC patients. PanC patients comprise a valid

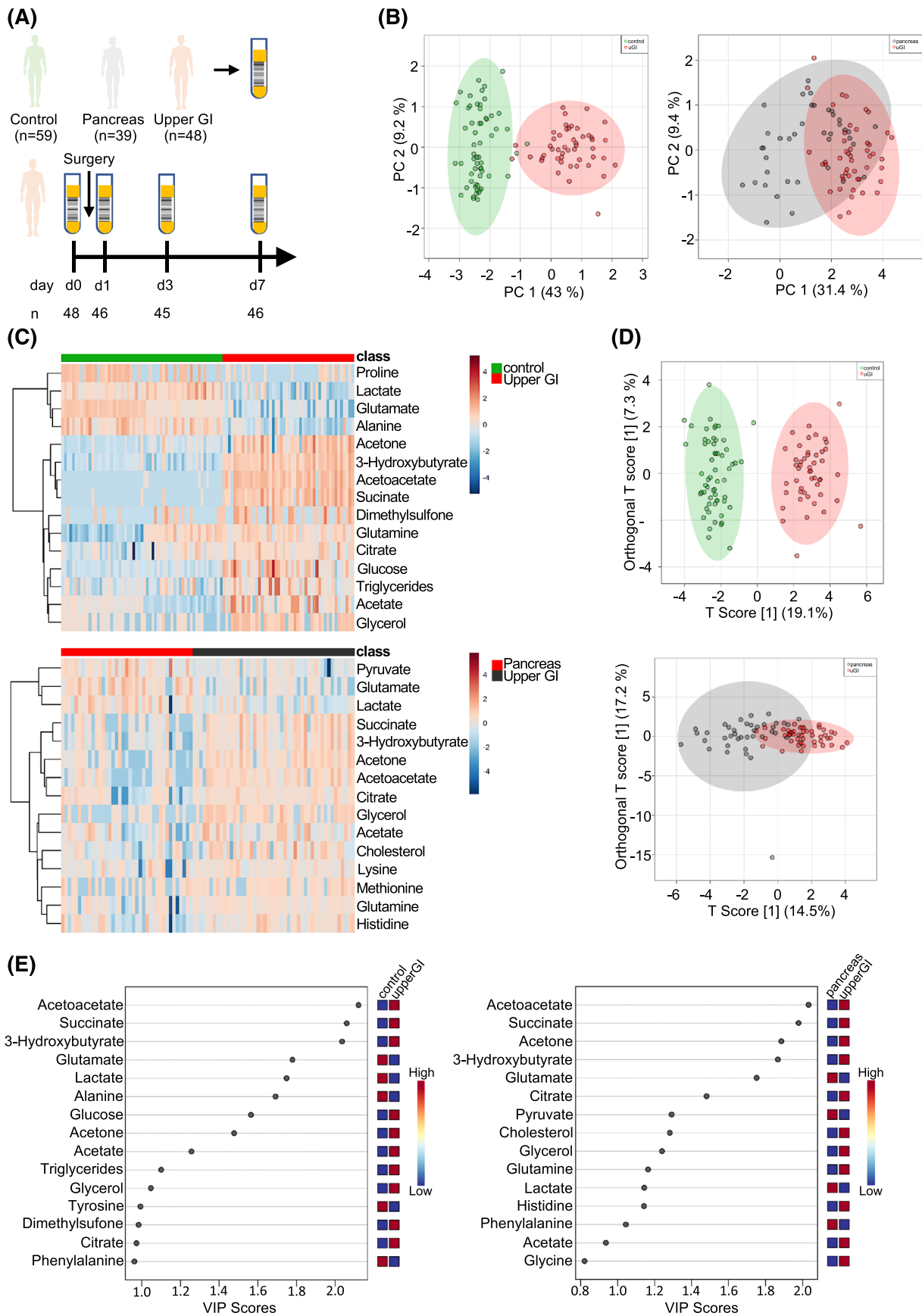


**Figure 1** Study design and metabolic profile. (A) Human cohort of 48 upper gastrointestinal (GI) cancer patients, 59 healthy controls, and 39 PanC control patients. Schematic timeline of the blood drawing protocol of 48 upper GI cancer patients before surgery (d0), the first postoperative day (d1), the third postoperative day (d3) and the seventh postoperative day (d7). (B) Principal component analysis (PCA) based on 42 metabolites identified by  $^1\text{H}$  NMR spectroscopy and calculated metabolite concentrations. Comparison of 48 upper GI cancer patients with 59 healthy controls in the left plot. The right plot represents a comparison of 48 upper GI cancer patients with 39 PanC patients before surgery. (C) Hierarchical clustering analysis of the metabolome of patients with cancer in the upper GI tract compared with healthy controls (upper panel) and hierarchical clustering analysis of the metabolome of patients with cancer in the upper GI tract compared with PanC patients before surgery (lower panel). Represented are the top 15 significantly changed metabolites (false discovery rate [FDR] adjusted  $P < 0.05$ ). Each column represents one sample, and each row represents one metabolite. Colour intensity in each cell represents the normalized metabolite level in the respective sample. (D) Orthogonal partial least squares discriminant analysis (OPLS-DA) of respective patients and control individuals. (E) Variable importance in projection (VIP) score for the identification of important metabolites identified by OPLS-DA comparing upper GI cancer patients with healthy controls (left panel) and upper GI cancer patients with PanC patients (right panel). The coloured boxes on the right indicate the relative concentrations of the corresponding metabolite in each group.

control group due to their similar age and pre-existing disease distribution. Additionally, the tumour location of PanC patients is close to the upper GI groups' and both cancer types are known for the appearance of cancer anorexia–cachexia syndrome (CACS). To follow the hypothesized normalization of cancer-related metabolic disruptions after surgery, we performed a metabolomic analysis with samples collected before and at three longitudinal time points after surgical resection.

Unsupervised PCA of the preoperative metabolome of 48 upper GI cancer patients and 59 healthy controls (Figure 1A) showed an excellent separation in the principal components space (Figure 1B, left panel). Interestingly, a clear separation trend was also achieved when the metabolomic signatures of the upper GI cancer patients were applied in the PCA against the metabolic marks in the sera of 39 PanC patients (Figure 1B, right panel). To exclude the presence of an inhomogeneous metabolic pattern which would argue against the combination of both cancer types in a single group, we also analysed both cancer types separately in an unsupervised PCA. As shown in Figure S1, the metabolic pattern of healthy controls nicely separated from oesophageal and gastric cancer patients, but there was no obvious separation between the two cancer types. Moreover, to exclude that the catabolic signature we identified was driven separately by a specific cancer subgroup, we performed an ANOVA multiple comparison analysis comparing the oesophageal and the gastric cancer patients separately with control or pancreatic cancer patients (Tables S2 and S3). In results, the ketone body dominated signature was significantly increased independently in the oesophageal and gastric subgroup compared with control or the PanC patients. Thus, the identified catabolic signature accounts for the overall upper GI cancer group (Tables S2 and S3).

Further, hierarchical clustering analysis (HCA) of 15 significantly altered serum metabolites (false discovery rate adjusted  $P < 0.05$ ) comparing upper GI cancer patients with healthy controls revealed severe alterations in ketone, amino acid, lipid and glucose metabolism (Figure 1C, upper panel). Similar metabolite classes were changed when comparing

serum metabolites of upper GI cancer patients with PanC patients (Figure 1C, lower panel).

Next, an OPLS-DA was employed to visualize group discrimination and consecutively calculate the separation driving metabolites in a VIP score. Metabolites that are responsible for the significant separation observed between the serum metabolome in healthy controls or PanC patients compared with upper GI cancer patients are indicated by a VIP score  $>1.0$ . OPLS-DA clearly separated upper GI cancer patients vs. healthy controls (Figure 1D, upper panel) and upper GI cancer vs. PanC patients (Figure 1D, lower panel). Interestingly, in both comparisons, driver metabolites ranking highest VIP scores were representatives of ketone and amino acid metabolism (Figure 1E).

### *Metabolomic analysis is consistent with a starvation status in the upper GI cancer patients*

The global trends that manifested in HCA and PCA before surgery prompted us to investigate nutrition-related metabolic alterations in upper GI cancer patients. After the initial discovery experiments, we focused on the comparison between upper GI and PanC patients. Pathway analysis confirmed that ketone metabolism was most strongly deregulated in upper GI cancer patients and amino acid and carbohydrate metabolism to a slightly lesser degree than in PanC patients (Figure 2A). Ketone body oxidation is best known to be induced upon fasting, starvation, and strict low-carbohydrate diets. Total ketone body concentrations can rise to approximately 1 mmol/L after extensive exercise or 24-h fasting.<sup>19</sup> Interestingly, the ketone bodies 3-hydroxybutyrate, acetoacetate and acetone were significantly elevated in upper GI cancer patient sera compared with PanC patients, with many upper GI cancer patients exceeding physiologic levels (Figure 1C lower panel, and Figure 2B). To exclude that the difference in ketone bodies between upper GI cancer and PanC patients was driven by an increased rate of neoadjuvant chemotherapy in upper GI cancer patients, we compared the metabolic signature of patients with and without neoadjuvant chemotherapy. No

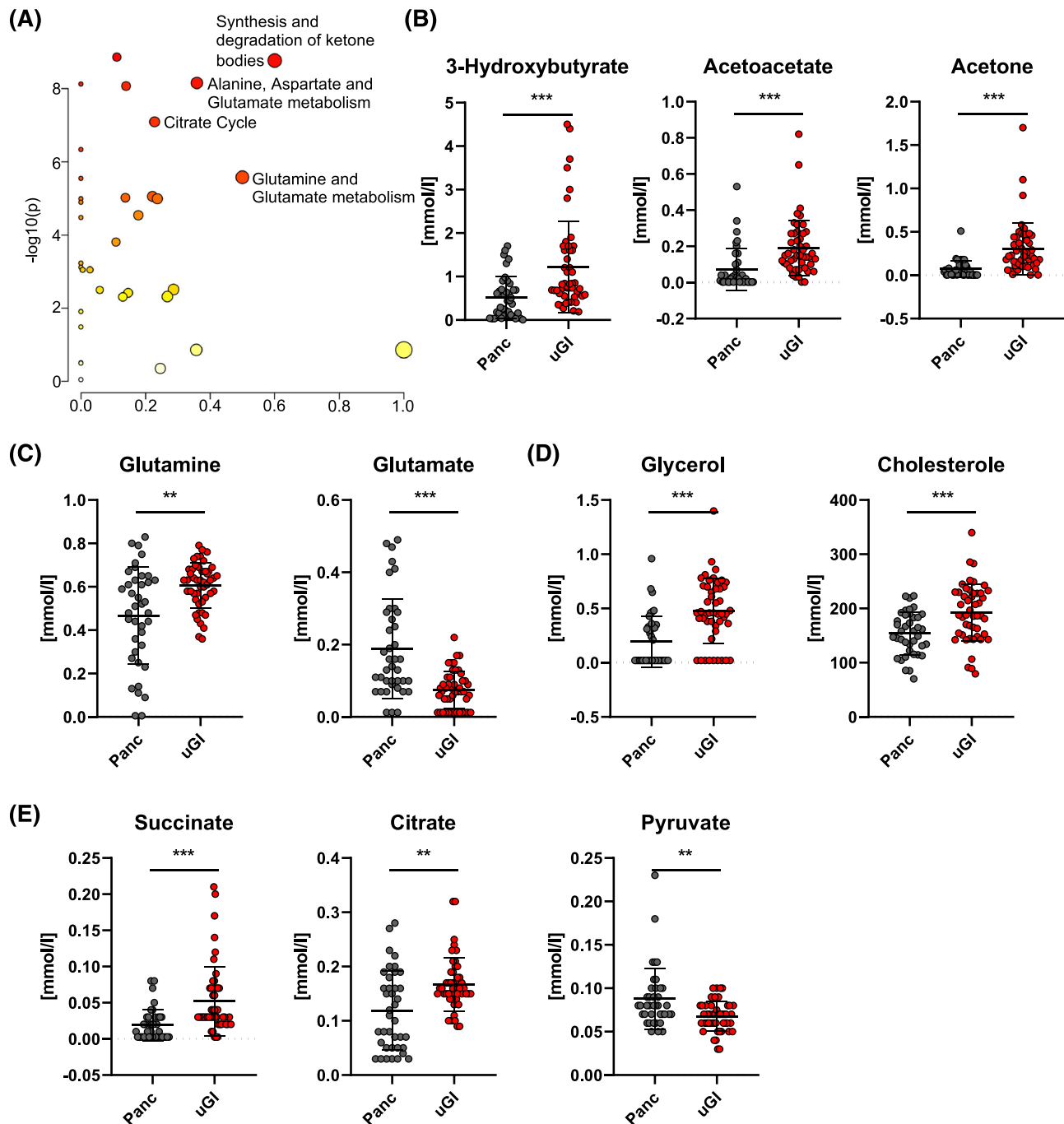


**Figure 2** Pathway analysis reveals starvation metabolism in upper gastrointestinal (GI) cancer patients. (A) Metabolic pathway analysis comparing the metabolome of upper GI cancer patients and PanC patients before surgery. The y-axis indicates pathway impact and the x-axis the statistical significance depicted as a log scale. Highlighted pathways were significantly altered in pathway analysis with  $P < 0.05$  and FDR of 1%. (B–E) Significantly altered metabolites involved in altered metabolic pathways. (B) Ketone bodies (3-hydroxybutyrate, acetoacetate, and acetone); (C) glutamine metabolism (glutamine and glutamate); (D) lipid metabolism (glycerol and cholesterol) as well as (E) citric acid cycle and carbohydrate metabolism (succinate, citrate and pyruvate).

difference was found in the concentration of analysed metabolites, demonstrating that neoadjuvant chemotherapy does not alter the upper GI cancer metabolomic signature (Figure S2).

For extrahepatic utilization, ketone bodies are broken down into acetyl-CoA moieties. Acetoacetate receives a CoA unit from Succinyl-CoA in the mitochondrial matrix, generating succinate<sup>20,21</sup> (Figure S3). Interestingly, peripheral

succinate levels were markedly increased in the peripheral blood of upper GI cancer patients (*Figure 1C* lower panel, *Figures 2E* and *S3*) compared with the concentrations obtained in PanC patients. Glycogen-deprived muscle tissue breaks down amino acids as an alternative fuel. The generated ammonia is fused with glutamate to synthesize glutamine. Glutamine is released into the bloodstream providing fuel for gluconeogenesis in the liver.<sup>22</sup> Consistently, upper GI cancer patients showed a substantial increase in glutamine concentration and decreased glutamate levels (*Figures 1D, 2C* and *S3*). The decreased concentration of lactate (primarily derived from skeletal muscle<sup>23</sup>) and pyruvate and the significantly increased glucose concentration might indicate insulin resistance in upper GI cancer patients compared with healthy controls. Although the underlying mechanisms are unknown, insulin resistance is suggested to be a risk factor for gastric cancer, as a prospective multicentre study has shown an association between insulin resistance and early gastric cancer.<sup>24</sup> In line with the increased abundance of ketones in the sera of upper GI cancer patients, metabolites linked to lipid utilization were also increased (*Figures 1D, 2D* and *S3*).

Adipose tissue triglycerides are hydrolyzed into glycerol and free fatty acids (FAs) and delivered through the bloodstream for  $\beta$ -oxidation and ketone body synthesis in the liver.<sup>25</sup> Indeed, glycerol was significantly elevated in upper GI cancer patients (*Figures 1D, 2D* and *S3*). Additionally, prolonged starvation is associated with cholesterol mobilization.<sup>26</sup> Total cholesterol was significantly increased in upper GI cancer patients compared with PanC patients' sera (*Figure 1C* lower panel, *Figure 2D*). Finally, the sera of upper GI cancer patients were enriched with citrate (*Figure 1C* lower panel, *Figures 2D* and *S3*), which has been shown to be increased in precachexic cancer patients compared with non-cachexic cancer patients of various aetiology.<sup>27</sup> Collectively, these data are indicative of convergence towards an adaptive starvation metabolism.

### *Ketosis is associated with amino acid catabolism*

Many cancer patients suffer from severe muscle loss associated with worse outcomes and poor quality of life.<sup>28</sup> Common scores like the NRS might miss subsets of patients that have catabolic metabolism before developing severe clinical symptoms.

We hypothesized that increased ketone body concentrations are associated with amino acid catabolism. Indeed, Pearson correlation coefficient showed a significant positive correlation between the branched-chain amino acids (BCAA) leucine and isoleucine that are mobilized from muscle tissue during prolonged starvation (*Figures 3A* and *S3*) with 3-hydroxybutyrate in upper GI cancer patients. Leucine is solely ketogenic, while isoleucine can feed both

gluconeogenesis and ketogenesis. Interestingly, alanine and pyruvate, which are substrates for gluconeogenesis in the liver, correlated negatively with 3-hydroxybutyrate (*Figures 3A* and *S3*).

In the absence of metabolic disturbances, 3-hydroxybutyrate levels remain below 1 mmol/L.<sup>20</sup> Higher levels have been shown to occur in metabolic disorders or after prolonged starvation for more than 24 h. Physiologically preoperative starvation does not induce ketosis (defined as 3-hydroxybutyrate levels above 1 mmol/L).<sup>29</sup> We addressed the question of whether ketosis is associated with increased amino acid breakdown by comparing upper GI cancer patients with preoperatively high and low 3-hydroxybutyrate levels (3-hydroxybutyrate >1 and <1) (*Figure 3C*). As expected, the solely ketogenic amino acid leucine and isoleucine, which can also support ketogenesis, were significantly increased in sera of ketotic patients. Cachexia is usually not characterized by ketosis. Accordingly, elevated 3-hydroxybutyrate levels were not associated with higher NRS scores (*Figure 3B*). Furthermore, clinical and laboratory parameters associated with cachexia or increased inflammatory states did not differ between ketosis and non-ketonemic upper GI cancer patients (*Figure S4A–E*). There was no difference in BMI, patient age and the analysis of C-reactive protein (CRP). Moreover, neither the number of leukocytes nor albumin serum levels that are decreased in cachexia<sup>30</sup> were dependent on the 3-hydroxybutyrate concentration (*Figure S4A,E*). In line with these findings, CRP/albumin and CRP/BMI ratios were also found to be independent of 3-hydroxybutyrate concentrations in plasma (*Figure S4F,G*). Together, patients with upper GI tumours show a catabolic metabolism that is not detected by classical indicators like the NRS score or albumin levels.

### *Surgical resection reverses metabolic dysregulation in upper GI cancer patients*

We hypothesized that preoperative metabolic alterations were tumour-induced and would resolve upon resection. To tackle this question, we assessed the postoperative longitudinal metabolic alterations by measuring the serum metabolome preoperatively and on the first, third and seventh postoperative days. Indeed, the patients' postoperative metabolic profile converged into a discrete cluster along PC1 clearly separated from the preoperative metabolic profile (*Figure 4A*). As expected, the most substantial changes were observed in metabolites that distinguished upper GI cancer patients from pancreatic patients and normal controls before surgery (*Figure 4B*). Ketone bodies quickly declined within 3 days after surgery. Physiological levels stabilized following Day 3, and no more significant changes were observed compared with Day 7 after surgery (*Figure 4C*).

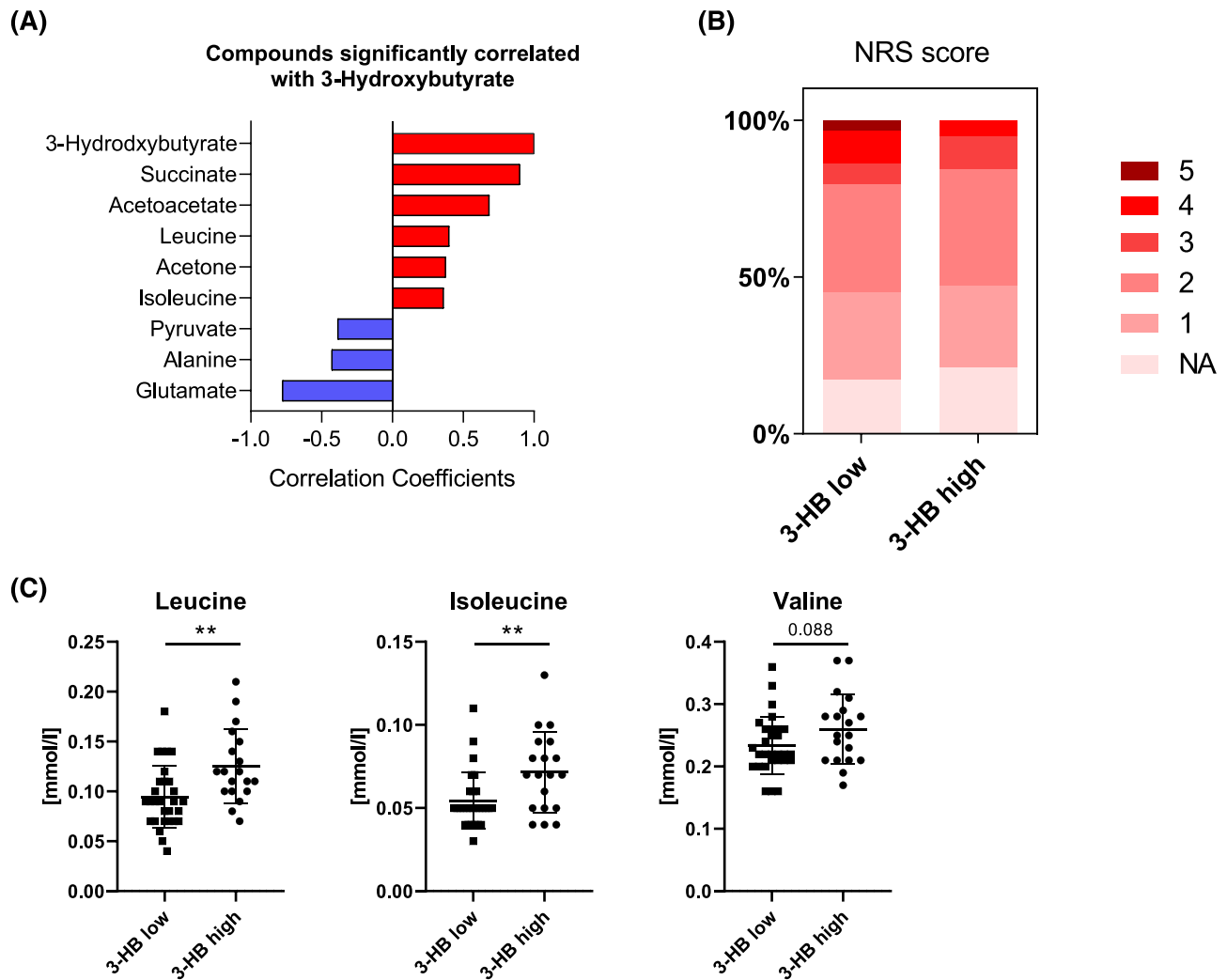


**Figure 3** Ketosis is associated with undetected catabolic amino acid metabolism. (A) Pearson correlation analysis of metabolites significantly correlating with 3-hydroxybutyrate in upper GI cancer patients before surgery ( $P < 0.05$ ). Red indicates positive and blue negative correlation. (B, C) patients from the upper GI cohort were separated based on 3-hydroxybutyrate (HB) levels into ketotic (3-hydroxybutyrate  $> 1.0$  mmol/L = 3-hydroxybutyrate high) and non-ketotic patients (3-hydroxybutyrate  $< 1.0$  mmol/L = 3-hydroxybutyrate low). (B) Comparison of percentages of patients' nutritional risk screening (NRS) scores in upper GI cancer 3-hydroxybutyrate high and upper GI cancer 3-hydroxybutyrate low patients. (C) Increased levels of branched-chain amino acid in the serum of 3-hydroxybutyrate high compared with 3-hydroxybutyrate low patients.

Succinate, possibly a product of peripheral tissue ketone utilization, paralleled the ketone body decline (Figure 4D). Cholesterol and the triglyceride backbone glycerol collectively decrease within 1 day after surgery, indicating a decrease of peripheral lipid mobilization<sup>26,31,32</sup> (Figure 4E). Surgery also led to a reduction of glutamine concentration, with a corresponding increase of glutamate (Figure 4E). In contrast, pyruvate demonstrated volatility with an initial concentration surge after surgery, followed by a drop on Day 3 and a second increase on Day 7 after surgery (Figure 4D).

Finally, we tested to what extent the metabolic signature of upper GI cancer patients 7 days after surgery has normalized by comparing it with the metabolic profile of healthy controls (Figure 4F). Strikingly, the PCA clearly revealed a

normalization of the metabolic profile towards the healthy control state. Collectively these longitudinal metabolomics data demonstrate a swift decline of cancer-induced metabolic disturbances by surgical resection.

## Discussion

In the present study, we discriminated 48 sera of upper GI cancer patients from 59 healthy controls and 39 PanC control patients using PCA and a multivariate OPLS-DA model and followed the metabolic changes longitudinally after tumour resection. Hereby, we could demonstrate for the first time that metabolic alterations quantified in sera of operated



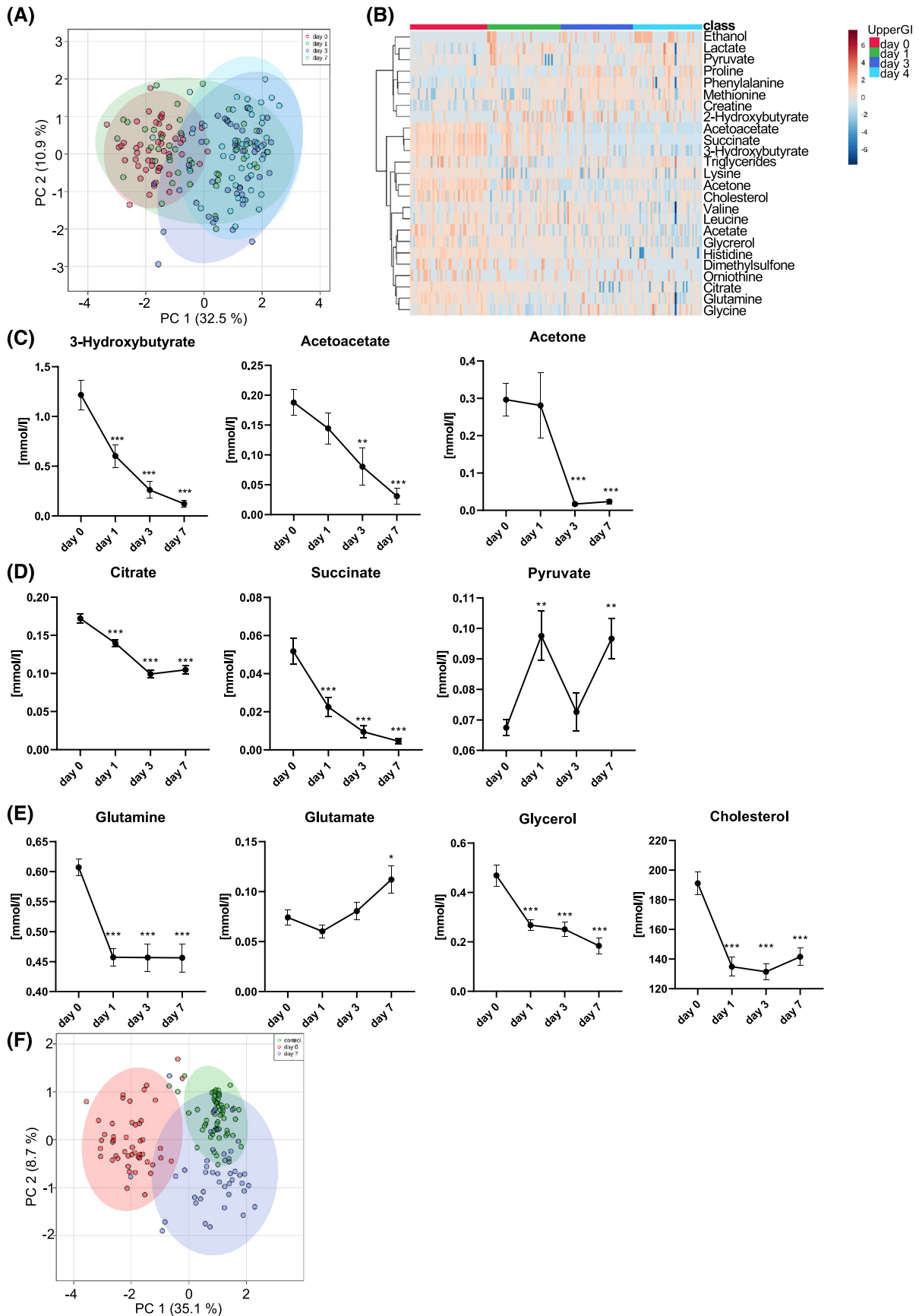


**Figure 4** Longitudinal metabolomics unravels sustained postoperative metabolic alterations. (A) Unsupervised PCA, showing the shift of the metabolic profile from before surgery (red) towards PC1 at the first postoperative day (green), and the metabolic stabilization at PC1 on Days 3 (dark blue) and 7 (bright blue) after surgery. (B) Heat map displaying hierarchical clustering analysis of relative metabolites concentrations in longitudinal profiles of 48 upper GI cancer patients. Twenty-four significantly altered metabolites are shown. Day 0 indicates blood drawing before surgery, followed by postoperative Days 1, 3 and 7. (C–F) Longitudinal metabolite concentration line plots of upper GI cancer patients of metabolites significantly altered over time and compared with PanC patients before surgery. Serum samples were measured before surgery (Day 0), on the first (Day 1), third (Day 3) and seventh (Day 7) after surgery. Analysis of metabolites involved in ketone body metabolism (C), citric acid cycle and carbohydrate metabolism (D) as well as glutamine and lipid metabolism (E). (F) Unsupervised PCA of the metabolomics measurements upper GI patients before surgery (red), at the seventh postoperative day (blue) and control patients (green).

upper GI cancer patients largely readjust within 7 days post-surgery, becoming indistinguishable from healthy controls.

We chose a metabolomics approach based on  $^1\text{H}$  NMR spectroscopy that allows for the absolute quantification of metabolite concentrations. Although mass spectrometry offers greater sensitivity and thus higher metabolite coverage,  $^1\text{H}$  NMR spectroscopy is characterized by high reproducibility due to standardized sample preparation, measurement and processing. Moreover, low-cost reagents and a simpler sample preparation compared with mass spectrometry keeping sample integrity intact enables affordable high-throughput metabolomics analyses. Thus,  $^1\text{H}$  NMR spectroscopy meets critical prerequisites for possible clinical application.

In order to identify a specific upper GI cancer signature in the serum, we did not only rely on serum of healthy controls but also included sera of patients with PanC, collected prior to surgery to reduce confounding effects. This additional cohort was chosen because approximately 80% of PanC patients suffer from CACS. Primary cachexia and anorexia caused by mechanical tumour obstruction are also common in upper GI cancer patients. Hence, PanC patients closely resemble upper GI cancer patients' nutritional status. First, we used an unsupervised PCA to extract meaningful patterns from the noise in the datasets and continued by employing a univariate statistical method combined with hierarchical clustering to identify characteristic metabolites in sera of upper GI cancer patients compared with healthy controls or PanC patients. This analysis strategy revealed expected differences between upper GI cancer patients and healthy controls but also a surprisingly similar metabolic pathway dysregulation compared with PanC patients. The multivariate statistical method (OPLS-DA) carried out afterward confirmed the results of the PCA.

Furthermore, the calculated VIP score was used to demonstrate the emphasis of key metabolites identified by OPLS-DA, which are responsible for the significant discrimination between the upper GI cancer patients and healthy controls or PanC patients, respectively. The obtained prominent serum ketone signature, characterized by an increased concentration of 3-hydroxybutyrate, acetoacetate and acetone in upper GI cancer patients compared with healthy controls, has been demonstrated previously.<sup>33</sup> Increased concentrations of ketones in serum have also been observed

in patients with colorectal malignancy, late-stage oral squamous cell carcinoma and lung cancer.<sup>34</sup> Because blood samples of upper GI cancer patients and PanC patients were obtained in the morning after overnight fasting, a starvation bias between the two groups was prevented. The production of ketones occurs mainly in the liver following FA beta-oxidation in response to increased lipolysis in adipose tissue. Although ketones are mainly consumed in skeletal muscle, heart and brain, increased ketone utilization in cancer tissue is equally possible. It has been shown that cancer cells can induce oxidation of ketones to fulfil their energetic demands in a low-glucose environment and promote cancer progression.<sup>35</sup>

Published results about ketone body concentrations in oesophageal and gastric cancer tissue are inconsistent. One group has reported increased concentrations compared with normal mucosa<sup>36</sup>; others found a significant downregulation.<sup>37</sup> Hence, it remains unclear if upper GI tumours metabolize ketones significantly.

A prerequisite for the observed ketosis in upper GI cancer patients is increased lipolysis in adipose tissue leading to an increased glycerol release, as we have observed in upper GI cancer patients compared with both healthy controls and PanC patients. The increased cholesterol levels in sera of upper GI cancer patients compared with PanC patients is a further sign of prolonged starvation because it has been shown that starvation triggers cholesterol release from lysosomes.<sup>38</sup> However, it cannot be excluded that the elevated cholesterol levels are a consequence of long-term overnutrition because studies have demonstrated a link between serum cholesterol levels and the risk for oesophageal and gastric cancer.<sup>39,40</sup> In line with the obtained ketone signature, the concentration of succinate, which is produced during the utilization of ketones, was increased in sera of upper GI cancer patients compared with healthy controls or PanC patients. Nonetheless, these elevated succinate levels could alternatively be a product of tumour cells or other sources.

The accumulation of glutamine in the plasma of upper GI patients and specifically BCAA in patients with ketosis is likely another consequence of prolonged malnutrition. Thus, the metabolic requirements in upper GI cancer patients drive proteolysis in skeletal muscle that delivers amino acids used

in gluconeogenesis and amino acids that support ketone biosynthesis in addition to FA degraded in beta-oxidation. However, as they feed into the TCA cycle, their metabolic fate might also be energy production by oxidative phosphorylation. Glutaminolysis increases in cancer because glutamine is catabolized to glutamate. The observed elevated glutamine abundance in sera of upper GI patients could consequently meet the increased energy requirements of cancer cells.

The surprisingly decreased concentrations of pyruvate and lactate together with the significantly increased glucose concentration point to an altered glucose homeostasis in upper GI cancer patients, at least compared with healthy controls. Many studies have shown a close association between diabetes and oesophageal or gastric cancer,<sup>41</sup> although it remains unclear whether insulin resistance increased the risk for upper GI cancer or if it is the other way around. However, results from the FIESTA study suggest that preoperative elevated blood glucose levels predict a poor prognosis for upper GI cancer patients.<sup>42</sup>

Strikingly our longitudinal data revealed that the ketone-dominated signature in upper GI cancer patients quickly disappeared after surgical tumour resection. Within 24 h and before (par)enteral nutrition was started, we observed a significant drop in 3-hydroxybutyrate, accompanied by a reduction in, for example, acetoacetate, succinate, glutamate, glycerol and cholesterol. Hence, our data suggest that surgical resection itself could sufficiently revert metabolic alterations, although patients were continued fasting overnight post-surgery. This suggests that the observed metabolic signature in sera of upper GI cancer patients is likely a primary consequence of tumour progression and is not only owing to secondary circumstances such as prolonged starvation due to, for example, mechanical obstruction.

In conclusion, quantifying the serum metabolic profile of patients with upper GI tumours using <sup>1</sup>H NMR spectroscopy resulted in the identification of an upper GI cancer-specific

signature driven by increased lipolysis, ketone biosynthesis, and amino acid depletion. Interestingly, its swift reversal after tumour resection revealed independence of malnutrition and inflammation and thus underlined the importance of longitudinal studies in addition to cross-sectional comparisons for enhanced data interpretation. Moreover, these data demonstrate the promising potential for serum metabolome analyses to control successful tumour resection and cancer recurrence. However, further analyses with larger patient cohorts are required to validate this observation.

## Acknowledgements

This study was supported by funds supporting a major research instrumentation from the National Center for Tumor Diseases (NCT), Partner Site Dresden, German Cancer Research Center (DKFZ), Heidelberg, Germany.

Open Access funding enabled and organized by Projekt DEAL.

## Conflict of interest

The authors declare no conflict of interest. The authors certify that they comply with the ethical guidelines for publishing in the *Journal of Cachexia, Sarcopenia and Muscle*, update: 2021.

## Online supplementary material

Additional supporting information may be found online in the Supporting Information section at the end of the article.

## References

1. Wong MCS, Huang J, Chan PSF, Choi P, Lao XQ, Chan SM, et al. Global incidence and mortality of gastric cancer, 1980–2018. *JAMA Netw Open* 2021;**4**:e2118457.
2. Arnold M, Abnet CC, Neale RE, Vignat J, Giovannucci EL, McGlynn KA, et al. Global burden of 5 major types of gastrointestinal cancer. *Gastroenterology* 2020;**159**:335–349, e15.
3. Schcolnik-Cabrera A, Chávez-Blanco A, Domínguez-Gómez G, Dueñas-González A. Understanding tumor anabolism and patient catabolism in cancer-associated cachexia. *Am J Cancer Res* 2017;**7**:1107.
4. Kudou K, Saeki H, Nakashima Y, Edahiro K, Korehisa S, Taniguchi D, et al. Prognostic significance of sarcopenia in patients with esophagogastric junction cancer or upper gastric cancer. *Ann Surg Oncol* 2017;**24**:1804–1810.
5. Bossi P, Delrio P, Mascheroni A, Zanetti M. The spectrum of malnutrition/cachexia/sarcopenia in oncology according to different cancer types and settings: A narrative review. *Nutrients* 2021;**13**:1980.
6. Shi B, Liu S, Chen J, Liu J, Luo Y, Long L, et al. Sarcopenia is associated with perioperative outcomes in gastric cancer patients undergoing gastrectomy. *Ann Nutr Metab* 2019;**75**:213–222.
7. Baracos VE, Martin L, Korc M, Guttridge DC, Fearon KCH. Cancer-associated cachexia. *Nat Rev Dis Primers* 2018;**4**:17105.
8. Arends J, Baracos V, Bertz H, Bozzetti F, Calder P, Deutz N, et al. ESPEN expert group recommendations for action against cancer-related malnutrition. *Clin Nutr* 2017;**36**:1187–1196.
9. Peixoto da Silva S, Santos JMO, Costa ESMP, Gil da Costa RM, Medeiros R. Cancer cachexia and its pathophysiology: links with sarcopenia, anorexia and asthenia.

- J Cachexia Sarcopenia Muscle* 2020;**11**: 619–635.
10. Horowitz M, Neeman E, Sharon E, Ben-Eliyahu S. Exploiting the critical peri-operative period to improve long-term cancer outcomes. *Nat Rev Clin Oncol* 2015;**12**:213–226.
  11. Kondrup J, Rasmussen HH, Hamberg O, Stanga Z, Group AahEW. Nutritional Risk Screening (NRS 2002): a new method based on an analysis of controlled clinical trials. *Clin Nutr* 2003;**22**:321–336.
  12. Sun Z, Kong XJ, Jing X, Deng RJ, Tian ZB. Nutritional risk screening 2002 as a predictor of postoperative outcomes in patients undergoing abdominal surgery: a systematic review and meta-analysis of prospective cohort studies. *PLoS ONE* 2015;**10**: e0132857.
  13. Freemark M. Metabolomics in nutrition research: biomarkers predicting mortality in children with severe acute malnutrition. *Food Nutr Bull* 2015;**36**:S88–S92.
  14. Huang S, Guo Y, Li Z, Zhang Y, Zhou T, You W, et al. A systematic review of metabolomic profiling of gastric cancer and esophageal cancer. *Cancer Biol Med* 2020;**17**:181–198.
  15. Dona AC, Jimenez B, Schafer H, Humpfer E, Spraul M, Lewis MR, et al. Precision high-throughput proton NMR spectroscopy of human urine, serum, and plasma for large-scale metabolic phenotyping. *Anal Chem* 2014;**86**:9887–9894.
  16. Pang Z, Chong J, Zhou G, de Lima Morais DA, Chang L, Barrette M, et al. MetaboAnalyst 5.0: narrowing the gap between raw spectra and functional insights. *Nucleic Acids Res* 2021;**49**:W388–W396.
  17. Do KT, Wahl S, Raffler J, Molnos S, Laimighofer M, Adamski J, et al. Characterization of missing values in untargeted MS-based metabolomics data and evaluation of missing data handling strategies. *Metabolomics* 2018;**14**:128.
  18. Chong J, Wishart DS, Xia J. Using MetaboAnalyst 4.0 for comprehensive and integrative metabolomics data analysis. *Curr Protoc Bioinformatics* 2019;**68**:e86.
  19. Cahill GF Jr. Fuel metabolism in starvation. *Annu Rev Nutr* 2006;**26**:1–22.
  20. Puchalska P, Crawford PA. Multi-dimensional roles of ketone bodies in fuel metabolism, signaling, and therapeutics. *Cell Metab* 2017;**25**:262–284.
  21. Watanabe S, Hirakawa A, Aoe S, Fukuda K, Muneta T. Basic ketone engine and booster glucose engine for energy production. *Diabetes Res Open J* 2016;**2**:14–23.
  22. He Y, Hakvoort TBM, Kohler SE, Vermeulen JLM, de Waart DR, de Theije C, et al. Glutamine synthetase in muscle is required for glutamine production during fasting and extrahepatic ammonia detoxification. *J Biol Chem* 2010;**285**:9516–9524.
  23. Juel C, Halestrap AP. Lactate transport in skeletal muscle—role and regulation of the monocarboxylate transporter. *J Physiol* 1999;**517**:633–642.
  24. Kwon HJ, Park MI, Park SJ, Moon W, Kim SE, Kim JH, et al. Insulin resistance is associated with early gastric cancer: a prospective multicenter case control study. *Gut Liver* 2019;**13**:154–160.
  25. Lee J, Choi J, Scafidi S, Wolfgang MJ. Hepatic fatty acid oxidation restrains systemic catabolism during starvation. *Cell Rep* 2016;**16**:201–212.
  26. Savendahl L, Underwood LE. Fasting increases serum total cholesterol, LDL cholesterol and apolipoprotein B in healthy, nonobese humans. *J Nutr* 1999;**129**:2005–2008.
  27. Yang QJ, Zhao JR, Hao J, Li B, Huo Y, Han YL, et al. Serum and urine metabolomics study reveals a distinct diagnostic model for cancer cachexia. *J Cachexia Sarcopenia Muscle* 2018;**9**:71–85.
  28. Aversa Z, Costelli P, Muscaritoli M. Cancer-induced muscle wasting: latest findings in prevention and treatment. *Ther Adv Med Oncol* 2017;**9**:369–382.
  29. Burstal R, Reilly J, Burstal B. Fasting or starving? Measurement of blood ketone levels in 100 fasted elective and emergency adult surgical patients at an Australian tertiary hospital. *Anaesth Intensive Care* 2018;**46**:463–467.
  30. Letilovic T, Perkov S, Mestric ZF, Vrhovac R. Differences in routine laboratory parameters related to cachexia between patients with hematological diseases and patients with solid tumors or heart failure—is there only one cachexia? *Nutr J* 2013;**12**:6.
  31. Stout RW, Henry RW, Buchanan KD. Triglyceride metabolism in acute starvation: the role of secretin and glucagon. *Eur J Clin Invest* 1976;**6**:179–185.
  32. Reshef L, Olswang Y, Cassuto H, Blum B, Croniger CM, Kalhan SC, et al. Glyceroneogenesis and the triglyceride/fatty acid cycle. *J Biol Chem* 2003;**278**: 30413–30416.
  33. Zhang X, Xu L, Shen J, Cao B, Cheng T, Zhao T, et al. Metabolic signatures of esophageal cancer: NMR-based metabolomics and UHPLC-based focused metabolomics of blood serum. *Biochim Biophys Acta* 2013;**1832**:1207–1216.
  34. Tiziani S, Lopes V, Günther UL. Early stage diagnosis of oral cancer using <sup>1</sup>H NMR-based metabolomics. *Neoplasia* 2009;**11**:269–276, 4p following 269.
  35. Bonuccelli G, Tsigiris A, Whitaker-Menezes D, Pavlides S, Pestell RG, Chiavarina B, et al. Ketones and lactate “fuel” tumor growth and metastasis: Evidence that epithelial cancer cells use oxidative mitochondrial metabolism. *Cell Cycle* 2010;**9**: 3506–3514.
  36. Reed MAC, Singhal R, Ludwig C, Carrigan JB, Ward DG, Taniere P, et al. Metabolomic evidence for a field effect in histologically normal and metaplastic tissues in patients with esophageal adenocarcinoma. *Neoplasia* 2017;**19**:165–174.
  37. Wang H, Zhang H, Deng P, Liu C, Li D, Jie H, et al. Tissue metabolic profiling of human gastric cancer assessed by <sup>1</sup>H NMR. *BMC Cancer* 2016;**16**:371.
  38. Eid W, Dauner K, Courtney KC, Gagnon A, Parks RJ, Sorisky A, et al. mTORC1 activates SREBP-2 by suppressing cholesterol trafficking to lysosomes in mammalian cells. *Proc Natl Acad Sci U S A* 2017;**114**: 7999–8004.
  39. Jin Y, Yang T, Li D, Ding W. Effect of dietary cholesterol intake on the risk of esophageal cancer: a meta-analysis. *J Int Med Res* 2019;**47**:4059–4068.
  40. Miao P, Guan L. Association of dietary cholesterol intake with risk of gastric cancer: a systematic review and meta-analysis of observational studies. *Front Nutr* 2021;**8**:722450.
  41. Cheng KC, Chen YL, Lai SW, Tsai PY, Sung FC. Risk of esophagus cancer in diabetes mellitus: a population-based case-control study in Taiwan. *BMC Gastroenterol* 2012;**12**:177.
  42. Hu D, Peng F, Lin X, Chen G, Liang B, Li C, et al. The elevated preoperative fasting blood glucose predicts a poor prognosis in patients with esophageal squamous cell carcinoma: The Fujian Prospective Investigation of Cancer (FIESTA) study. *Oncotarget* 2016;**7**:65247–65256.